Depth Resolution in Coherent Hemodynamics Spectroscopy

Angelo Sassaroli, Xuan Zang, Kristen T. Tgavalekos and Sergio Fantini
Department of Biomedical Engineering, Tufts University, 4 Colby Street, MA 02155, Medford, U.S.A.

Keywords: Near-infrared Spectroscopy, Diffuse Optics, Diffusion Theory, Functional Optical Imaging, Cerebral Hemodynamics.

Abstract: Coherent hemodynamics spectroscopy (CHS) is a novel method based on the frequency-resolved study of induced hemodynamic oscillations in living tissues. Approaches to induce hemodynamic oscillations in human subjects include paced breathing and cyclic thigh cuff inflation. Such induced hemodynamic oscillations result in coherent oscillations of oxy-, deoxy-, and total hemoglobin concentrations in tissue, which can be measured with near-infrared spectroscopy (NIRS). The novel aspect of CHS is to induce hemodynamic oscillations at multiple frequencies in order to obtain frequency-resolved spectra of coherent hemodynamics. A dedicated mathematical model recently developed by our group, can translate the phase and amplitude spectra of these hemodynamic oscillations into physiological parameters such as capillary and venous transit times, and the autoregulation cutoff frequency. A typical method used in near-infrared tissue spectroscopy to measure oscillations of hemoglobin concentrations is based on the modified Beer-Lambert law, which does not allow for the discrimination of hemodynamic oscillations occurring in the scalp from those occurring in the brain cortex. In this work, we show preliminary results obtained by using diffusion theory for a two-layered medium, so that the hemodynamic oscillations obtained for the first and second layer are assigned to hemodynamic oscillations occurring in the scalp/skull and brain cortex tissues, respectively.

1 INTRODUCTION

Most neuroimaging techniques, with the exception of electroencephalography (EEG) and electrophysiological techniques, do not measure directly neural activation but rather measure some associated hemodynamic responses. Among these neuroimaging techniques we mention: functional magnetic resonance imaging (fMRI), positron emission tomography (PET), single-photon emission computed tomography (SPECT) and near infrared spectroscopy (NIRS). Therefore, in order to obtain an assessment of brain function by these neuroimaging techniques, it is of the utmost importance to understand the relationship between neural activation and hemodynamic changes (neurovascular coupling). Several hemodynamic models have been proposed in the literature, among which we mention the oxygen diffusion limitation model (Buxton and Frank, 1997), and the Windkessel model (Mandeville et al., 1999). The former was introduced in order to understand the large imbalance (observed in PET studies) between blood flow and oxygen consumption changes associated with brain activation. The latter was introduced to understand the relationship between the dynamics of blood flow and blood volume (measured by fMRI) during forepaw stimulation in rats. These general models can be used and adapted to each neuroimaging technique, which is sensitive to different physiological parameters.

Near-infrared spectroscopy (NIRS) is a non-invasive optical method which relies on the so-called diagnostic window of tissue transparency in the wavelength range 600-900 nm. In this wavelength range, the main absorbers in tissue are oxy-hemoglobin, deoxy-hemoglobin, water, and lipids. Recently, there has been a rapid growth of applications where NIRS is used, mainly due to its portability and continuous monitoring of tissue, which are unique assets of this optical method. Many hemodynamic models have been proposed also in NIRS, most of them requiring the solution of complex system of differential equations with many unknown parameters (Huppert et al., 2007; Diamond et al., 2009; Boas et al., 2008).

Sassaroli, A., Zang, X., Tgavalekos, K. and Fantini, S.
Depth Resolution in Coherent Hemodynamics Spectroscopy.
DOI: 10.5220/0005792101850191
In *Proceedings of the 4th International Conference on Photonics, Optics and Laser Technology (PHOTOPTICS 2016)*, pages 187-193
ISBN: 978-989-758-174-8

Recently, we proposed a novel technique to study tissue hemodynamics, named coherent hemodynamics spectroscopy (CHS) (Fantini, 2014a; Fantini, 2014b). The technique is based on inducing stable hemodynamic oscillations by introducing controlled, periodic perturbations (e.g. by paced breathing, cyclic thigh cuff inflation/deflation, etc.) at multiple frequencies. We also developed a mathematical hemodynamic model to translate the hemoglobin oscillations caused by the periodic perturbations, as measured by NIRS, into blood flow, blood volume, and oxidative metabolism dynamics. The mathematical model is analytical, and therefore simpler and less computationally expensive than other models proposed in the NIRS literature. The output variables of our analytical model are four: 1) the phase difference of deoxy- and oxy-hemoglobin oscillations; 2) the phase difference of oxy- and total hemoglobin oscillations; 3) the ratio of amplitudes of deoxy- and oxy-hemoglobin oscillations; 4) the ratio of amplitudes of oxy- and total hemoglobin oscillations. The model depends on six unknown parameters which are fitted for when the model is applied to experimental data. Among these unknown parameters, there are the capillary and venous blood transit times, and the autoregulation cutoff frequency, which provides a quantitative measure of cerebral autoregulation efficiency. In fact, we remind that most studies, both in transcranial Doppler ultrasound (TCD) and NIRS, treat the process of cerebral autoregulation as a high-pass filter, where blood pressure is the input and cerebral blood flow is the output of the filter. Our analytical model has been tested in several experimental studies on healthy human subjects (Pierro et al., 2014a; Kainerstorfer et al., 2015) and on hemodialysis patients (Pierro et al., 2014b).

In NIRS, the oscillations of oxy- and deoxy-hemoglobin concentrations are usually derived by applying the modified Beer-Lambert law (mBLL) to the intensity changes measured at two (or more) wavelengths. The mBLL, unlike the diffusion equation, which is also used to study photon migration in tissues, does not require the medium to be highly scattering (Sassaroli and Fantini, 2004). However, the mBLL is based on two assumptions: 1) the changes of optical intensity are due only to absorption changes; 2) the changes in absorption are homogeneously distributed in the tissue probed by light. While the first assumption is reasonable, the second one is more questionable. For example, it is well known that brain activation and subsequent hemodynamic changes are focal in nature. Therefore, it would be important to release the assumption of homogeneous absorption changes and use a model of light propagation which takes into account (at least partially) the more complex geometry of the human head and of the heterogeneous hemodynamic changes associated with brain perfusion. The human head is a layered biological medium with scalp, skull, subarachnoid space, and the brain cortex (grey matter) as its "layers." In the literature, a two-layered diffusion model has been used for measuring the baseline optical properties of two "effective" layers of the head, where the first layer is representative of the scalp and the skull, lumped in one layer, and the second layer represents the brain (Choi et al, 2004; Gagnon et al, 2008; Hallacoglu et al., 2013). In this work, we have obtained the dynamics of oxy- and deoxy-hemoglobin concentrations by applying the solution of the diffusion equation in the frequency domain for a two-layer model medium. To the best of our knowledge, it is the first time that such a model is applied to calculate the dynamics of oxy- and deoxy-hemoglobin concentrations. The oscillations of oxy- and deoxy-hemoglobin concentrations induced at a frequency of 0.067 Hz, by means of a cyclic thigh cuff occlusion/release protocol, are calculated by using both the mBLL at three different source-detector separations and the two-layer diffusion model. In particular, we show that the phase difference between deoxy- and oxy-hemoglobin oscillations depends on the source-detector separation when the mBLL is used, and is different than the phase values retrieved by the two-layer model in the top and bottom layers.

2 MATERIALS AND METHODS

2.1 Experimental Setup

The NIRS measurements were performed with a commercial frequency-domain tissue spectrometer (OxiplexTS, ISS Inc., Champaign, IL). The laser intensity outputs were modulated at a frequency of 110 MHz. An optical probe connected to the spectrometer by optical fibers delivered light at two wavelengths, 690 and 830 nm, at six different locations, separated by a single collection optical fiber by: 7.3, 12.3, 17.6, 27.5, 32.8, 38.1 mm (690 nm) and 8.0, 13.2, 18.1, 28.1, 33.4, 37.3 mm (830 nm). The optical probe was placed against the left side of the subject's forehead and secured with a flexible headband. The optical instrument was calibrated by using an optical phantom of known

optical properties (Fantini et al., 1995). Pneumatic thigh cuffs were wrapped around both subject's thighs and connected to an automated cuff inflation system (E-20 Rapid Cuff Inflation System, D.E. Hokanson, Inc., Bellevue, WA). The air pressure in the thigh cuffs was continuously monitored with a digital manometer (Series 626 Pressure Transmitter, Dwyer Instruments, Inc., Michigan City, IN). Analog outputs of the thigh cuff pressure monitor were fed to auxiliary inputs of the NIRS instrument for concurrent recordings with the NIRS data. The subject underwent a protocol of eight cycles, where in each cycle the thigh cuff was inflated at a pressure of 200 mmHg for 8 s and released for 7 s. The method of analytic signal (Boashash, 1992; Pierro et al., 2012) was used to associate an average phase and amplitude to the oscillations of oxy-, deoxy-, and total hemoglobin concentrations. In other words, the oscillations of oxy-, deoxy-, and total hemoglobin concentrations are described with phasors, polar vectors whose amplitude and phase fully describe sinusoidal oscillations at a given frequency.

2.2 Hemodynamic Model

The hemodynamic model links the phasors representing the oscillations of blood flow, blood volume, and metabolic rate of oxygen to the phasors representing the oscillations of oxy-, deoxy-, and total hemoglobin concentrations. In the following Eqs. (1)-(3), $\mathbf{O}(\omega)$, $\mathbf{D}(\omega)$, $\mathbf{T}(\omega)$ are the phasors that describe the oscillations of oxy-, deoxy-, and total hemoglobin concentrations, which are functions of the oscillation angular frequency ω. Also, **cbv**(ω), **cbf**(ω), and $\mathbf{cmro_2}(\omega)$ are the phasors that describe the oscillations of cerebral blood volume, blood flow, and metabolic rate of oxygen, respectively. The model equations are as follows:

$$\begin{aligned}\mathbf{O}(\omega) = \mathrm{ctHb}\big[&S^{(a)}\mathrm{CBV}_0^{(a)}\mathbf{cbv}^{(a)}(\omega) \\ &+ S^{(v)}\mathrm{CBV}_0^{(v)}\mathbf{cbv}^{(v)}(\omega)\big] \\ &+ \mathrm{ctHb} \\ \times\Bigg[&\frac{\langle S^{(c)}\rangle}{S^{(v)}}\big(\langle S^{(c)}\rangle - S^{(v)}\big)\mathrm{F}^{(c)}\mathrm{CBV}_0^{(c)}\mathcal{H}_{RC-LP}^{(c)}(\omega) \\ &+ \big(S^{(a)} - S^{(v)}\big)\mathrm{CBV}_0^{(v)}\mathcal{H}_{G-LP}^{(v)}(\omega)\Bigg]\big[\mathbf{cbf}(\omega) \\ &- \mathbf{cmro_2}(\omega)\big]\end{aligned} \tag{1}$$

$$\begin{aligned}\mathbf{D}(\omega) = \mathrm{ctHb}\big[&\big(1 - S^{(a)}\big)\mathrm{CBV}_0^{(a)}\mathbf{cbv}^{(a)}(\omega) \\ &+ \big(1 - S^{(v)}\big)\mathrm{CBV}_0^{(v)}\mathbf{cbv}^{(v)}(\omega)\big] \\ &- \mathrm{ctHb} \\ \times\Bigg[&\frac{\langle S^{(c)}\rangle}{S^{(v)}}\big(\langle S^{(c)}\rangle - S^{(v)}\big)\mathrm{F}^{(c)}\mathrm{CBV}_0^{(c)}\mathcal{H}_{RC-LP}^{(c)}(\omega) \\ &+ \big(S^{(a)} - S^{(v)}\big)\mathrm{CBV}_0^{(v)}\mathcal{H}_{G-LP}^{(v)}(\omega)\Bigg]\big[\mathbf{cbf}(\omega) \\ &- \mathbf{cmro_2}(\omega)\big]\end{aligned} \tag{2}$$

$$\begin{aligned}\mathbf{T}(\omega) = \mathrm{ctHb}\big[&\mathrm{CBV}_0^{(a)}\mathbf{cbv}^{(a)}(\omega) \\ &+ \mathrm{CBV}_0^{(v)}\mathbf{cbv}^{(v)}(\omega)\big]\end{aligned} \tag{3}$$

In Eqs. (1)-(3), ctHb is the hemoglobin concentration in blood, $\mathrm{F}^{(c)}$ is the Fåhraeus factor (ratio of capillary-to-large vessel hematocrit), and the superscripts (a), (c), and (v) indicate partial contributions from the arterial, capillary, and venous compartments, respectively, to the baseline blood volume (CBV_0) and the oscillatory blood volume (**cbv**). The total baseline blood volume is defined by: $\mathrm{CBV}_0 = \mathrm{CBV}_0^{(a)} + \mathrm{F}^{(c)}\mathrm{CBV}_0^{(c)} + \mathrm{CBV}_0^{(v)}$. Also, $S^{(a)}$, $\langle S^{(c)}\rangle$, and $S^{(v)}$ are the arterial, mean capillary, and venous saturation. The mean capillary and venous saturations are given by $\langle S^{(c)}\rangle = S^{(a)}\left(1 - e^{-\alpha t^{(c)}}\right)/\left(\alpha t^{(c)}\right)$ and $S^{(v)} = S^{(a)}e^{-\alpha t^{(c)}}$ where α is the rate constant of oxygen diffusion and $t^{(c)}$ is the mean transit time of blood in the capillaries. The capillary ($\mathcal{H}_{RC-LP}^{(c)}(\omega)$) and venous ($\mathcal{H}_{G-LP}^{(v)}(\omega)$) transfer functions are represented by the following Eq. (4) and Eq. (5), respectively:

$$\mathcal{H}_{RC-LP}^{(c)}(\omega) = \frac{1}{\sqrt{1 + \left(\frac{\omega t^{(c)}}{e}\right)^2}} e^{-i\tan^{-1}\left(\frac{\omega t^{(c)}}{e}\right)} \tag{4}$$

$$\mathcal{H}_{G-LP}^{(v)}(\omega) = e^{-\frac{\ln 2}{2}\left[\omega\, 0.281\left(t^{(c)} + t^{(v)}\right)\right]^2} e^{-i\omega\, 0.5\left(t^{(c)} + t^{(v)}\right)} \tag{5}$$

where $t^{(v)}$ in Eq. (5) is the blood venous transit time. According to our hemodynamic model, only the capillary and venous compartments contribute to hemoglobin oscillations caused by oscillations of capillary blood flow and cerebral metabolic rate of oxygen. On the contrary, because capillary recruitment in the brain is negligible (Villringer, 2012) only the arterial and venous compartments can contribute to hemoglobin oscillations caused by blood volume oscillations. In particular, our model

predicts that the capillary and venous compartments behave as low pass filters having **cbf**, $\mathbf{cmro_2}$ as inputs, and **O**, **D**, **T** as outputs. Finally, the oscillations of blood flow are related to those of blood volume through a high-pass relationship typical of the autoregulation process:

$$\begin{aligned}\mathbf{cbf}(\omega) &= k\,\mathcal{H}_{RC-HP}^{(\mathrm{AutoReg})}(\omega)\mathbf{cbv}(\omega)\\ &= k\,\mathcal{H}_{RC-HP}^{(\mathrm{AutoReg})}(\omega)\\ &\times\left[\frac{\mathrm{CBV}_0^{(a)}}{\mathrm{CBV}_0}\mathbf{cbv}^{(a)}(\omega)+\frac{\mathrm{CBV}_0^{(v)}}{\mathrm{CBV}_0}\mathbf{cbv}^{(v)}(\omega)\right]\end{aligned} \quad (6)$$

In Eq. (6), k is the inverse of the modified Grubb's exponent and $\mathcal{H}_{RC-HP}^{(\mathrm{AutoReg})}(\omega)$ is the RC high pass filter having as input the weighted average of arterial and venous blood volume oscillations, and as output the capillary blood flow oscillations. The expression of $\mathcal{H}_{RC-HP}^{(\mathrm{AutoReg})}$ is as follows:

$$\mathcal{H}_{RC-HP}^{(\mathrm{AutoReg})}(\omega) = \frac{1}{\sqrt{1+\left(\frac{\omega_c^{(\mathrm{AutoReg})}}{\omega}\right)^2}}e^{\,i\tan^{-1}\left(\frac{\omega_c^{(\mathrm{AutoReg})}}{\omega}\right)} \quad (7)$$

In Eq. (7), $\omega_c^{(\mathrm{AutoReg})} = 2\pi f_c^{(\mathrm{AutoReg})}$ and $f_c^{(\mathrm{AutoReg})}$ is the autoregulation cutoff frequency.

2.3 Solution of the Diffusion Equation in a Two-Layer Cylindrical Geometry

A two-layer diffusive medium is divided into a top region (first layer) and bottom region (second layer) that are separated by a planar surface. The two media have different optical properties, namely the absorption coefficient (μ_a) and the reduced scattering coefficient (μ_s'). The diffusion equation in the frequency domain (FD) is written as:

$$\begin{aligned}&\nabla\cdot[D_0(\mathbf{r})\nabla\phi(\mathbf{r},\Omega)]-\left[\mu_a(\mathbf{r})+i\frac{\Omega}{v}\right]\phi(\mathbf{r},\Omega)\\ &=-P_{AC}(\Omega)\delta(\mathbf{r})\end{aligned} \quad (8)$$

In Eq.(8) ϕ is the fluence rate, i.e. the power per unit area impinging from all directions (units: W/m^2) at an arbitrary field point inside the medium (**r**); $D_0 = 1/(3\mu_s')$ is the diffusion coefficient, v is the speed of light in the medium, Ω is the angular modulation frequency of the light intensity (in this study $\Omega/(2\pi)$ is 110 MHz), δ is the Dirac delta, and P_{AC} is the source power. For the solution of Eq. (8) in a two-layered cylindrical medium, we have followed the approach of Liemert and Kienle (Liemert and Kienle, 2010). For a point source incident at the center of a layered cylindrical medium, the general solution of the two-layer diffusion equation in cylindrical coordinates (**r**=(ρ,θ,*z*); *z* is the direction of the cylinder's axis pointing inside the medium) is given by (Liemert and Kienle, 2010):

$$\begin{aligned}&\phi_k(\mathbf{r},\Omega)\\ &=\frac{P_{AC}(\Omega)}{\pi a'^2}\sum_{n=1}^{\infty}G_k(s_n,z,\Omega)J_0(s_n\rho)J_1^{-2}(a's_n)\end{aligned} \quad (9)$$

where ϕ_k is the fluence rate in the k^{th} layer of the medium (k = 1,2), s_n are the positive roots of the 0$^{\mathrm{th}}$-order Bessel function of the first kind divided by $a' = a + z_b$, (where a is the radius of the cylinder), and J_m is the Bessel function of the first kind of order m. Also, z_b is the distance between the extrapolated and the real boundary, $z_b = 2D_{01}(1+R_{\mathrm{eff}})/(1-R_{\mathrm{eff}})$, R_{eff} is the fraction of photons that are internally diffusely reflected at the cylinder boundary and D_{01} is the diffusion coefficient in the first layer. Here, we report the solution for G_k only for the first layer (k = 1), since it is the layer where the reflectance is calculated. For the first layer (the one illuminated by the light source), G_1 is given by the following expression:

$$\begin{aligned}&G_1(s_n,z,\Omega)\\ &=\frac{\exp(-\alpha_1|z-z_0|)-\exp[\alpha_1(z+z_0+2z_b)]}{2D_{01}\alpha_1}\\ &+\frac{\sinh[\alpha_1(z_0+z_b)]\sinh[\alpha_1(z+z_b)]}{D_{01}\alpha_1\exp[\alpha_1(L+z_b)]}\\ &\times\frac{D_{01}\alpha_1-D_{02}\alpha_2}{D_{01}\alpha_1\cosh[\alpha_1(L+z_b)]+D_{02}\alpha_2\sinh[\alpha_1(L+z_b)]}\end{aligned} \quad (10)$$

where L is the thickness of the first layer, and α_k is given by:

$$\alpha_k=\sqrt{\frac{\mu_{ak}}{D_{0k}}+s_n^{\,2}+\frac{i\Omega}{D_{0k}v}}\quad k=1,2 \quad (11)$$

Equation (10) is obtained for the limiting case when the second layer is infinite in the z direction and for the case of two layers having the same refractive indices (Liemert and Kienle, 2010). In Eq. (11), D_{0k} and μ_{ak} are the diffusion coefficient and the absorption coefficient of the k^{th} layer, respectively. For the calculation of the reflectance (R), one may apply Fick's law:

$$R(\rho,\Omega)=D_{01}\frac{\partial}{\partial z}\phi_1(\rho,z,\Omega)\Big|_{z=0} \quad (12)$$

From the expression of the reflectance (which is a complex function), we can calculate the AC(ρ,Ω) and phase θ(ρ,Ω) as follows: AC(ρ,Ω) = |R(ρ,Ω)|, θ(ρ,Ω) = Arg[R(ρ,Ω)]. The solution of the diffusion equation presented in this section was embedded in an inversion procedure which used the Levenberg-Marquardt method and that recovers the optical properties (μ_a, μ_s') of the two layers and the thickness of the first layer from measured AC and phase (Φ) data at six source detector separations (Hallacoglu et al., 2013). The inversion procedure is run at each time point. By combining the dynamics of the absorption coefficients retrieved by the inversion procedure at two wavelengths, we were able to calculate the dynamics of oxy- and deoxy-hemoglobin concentrations in the first and second layer.

3 RESULTS

Figure 1 shows the thigh cuff pressure oscillations (top panel) and the oscillations of oxy- (ΔO) and deoxy-hemoglobin (ΔD) concentrations induced by the cuff at three different source-detector separations. More precisely, the oscillations of oxy- and deoxy-hemoglobin concentrations were calculated according to the modified Beer-Lambert law (mBLL) by using the combined intensity oscillations at the first, third, and sixth source-detector separations (~8, 18, 38 mm, respectively). The temporal trends of ΔO and ΔD plotted in Fig. 1 are related to the phasors **O**(ω) and **D**(ω) (see Eqs. (1) and (2)) by the relationships: $\Delta O = \mathrm{Re}[|\mathbf{O}|e^{i\mathrm{Arg}(\mathbf{O})}e^{i\omega t}]$, $\Delta D = \mathrm{Re}[|\mathbf{D}|e^{i\mathrm{Arg}(\mathbf{D})}e^{i\omega t}]$ where ω is the angular frequency of the cuff cyclic inflation. The phase shift between deoxy- and oxy-hemoglobin oscillations (Arg(**D**)-Arg(**O**)) are: 106°±8°, 74°±8° and 68°±1° at the first, third, and sixth source-detector separations, respectively.

In Fig. 2, we report the thigh cuff pressure oscillations (top panel) and the oscillations of oxy- (ΔO) and deoxy-hemoglobin (ΔD) concentrations calculated by using the two-layer model. The phase shifts between deoxy- and oxy-hemoglobin oscillations (Arg(**D**)-Arg(**O**)) are: 24°±7° and 34°±9° in the top and bottom layers, respectively.

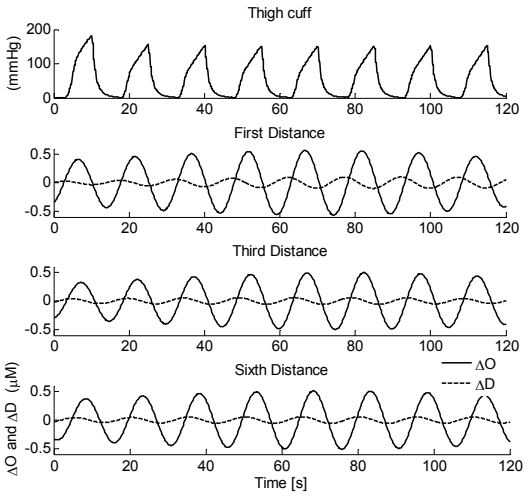

Figure1: Oscillations of the cuff pressure (top panel) and oscillations of ΔO and ΔD at the first (~8 mm: second panel) third (~18 mm: third panel) and sixth (~38 mm: bottom panel) source-detector separations, calculated by using the modified Beer-Lambert law (mBLL). The phase differences between deoxy- and oxy-hemoglobin oscillations (Arg(**D**)-Arg(**O**)) are 106°±8°, 74°±8° and 68°±1° at the first, third, and sixth source-detector separations, respectively.

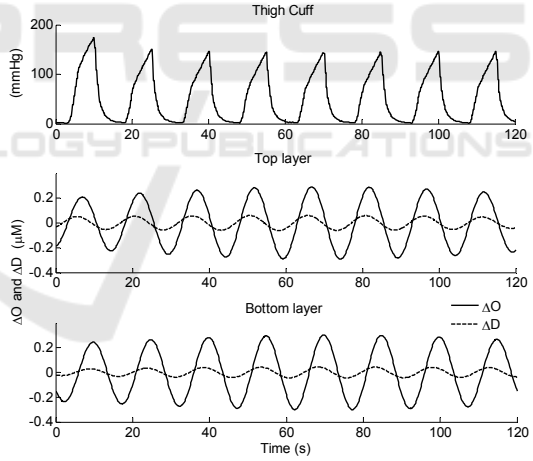

Figure 2: Oscillations of the cuff pressure (top panel) and oscillations of ΔO and ΔD in the top (second panel) and bottom (third panel) layers, calculated by using the two-layer model. The phase differences between deoxy- and oxy-hemoglobin oscillations (Arg(**D**)-Arg(**O**)) are 24°±7° and 34°±9° in the top and bottom layers, respectively.

4 DISCUSSIONS AND CONCLUSIONS

We have presented some preliminary results about the possibility of using a two-layer diffusion model

to provide depth resolution to measured oscillations of oxy- and deoxy-hemoglobin concentrations. In the literature, the two-layer diffusion model has already been used for the calculation of the baseline optical properties and hemoglobin concentrations in the two "effective" head tissue layers. To the best of our knowledge, this is the first time that such a model is used for the calculation of hemoglobin concentration oscillations. Typically, in NIRS the dynamics of hemoglobin species are calculated by using the modified Beer-Lambert law (mBLL), which assumes homogeneous absorption changes in the tissue probed by light. Since this hypothesis may not be strictly correct in a variety of conditions, it would be of the utmost importance to discriminate the hemodynamic oscillations occurring in the extracerebral layers (scalp and skull) from those occurring in the brain. For this reason, we have considered a more realistic model of the head which comprises two distinct layers. The solution of the diffusion equation in the FD for a two-layer geometry was implemented in an inversion procedure which recovers the dynamics of the absorption and reduced scattering coefficients of both layers, as well as the thickness of the first layer, from measured AC and phase data at six source-detector separations. We have calculated the phase shifts between oxy- and deoxy-hemoglobin oscillations with the two-layer model, and compared the results with those obtained with the mBLL at three different source detector separations. Our hemodynamic model (Eqs. (1)-(3)) shows that the phase shift between deoxy- and oxy-hemoglobin concentration is one of the parameters related to the dynamics of blood volume, blood flow and oxygen consumption and to the underlying physiological quantities of diagnostic and functional value (i.e. the capillary and venous blood transit times, the autoregulation cutoff frequency, etc.). Therefore, different phase shifts indicate different dynamics of the underlying vascular, metabolic, and physiological parameters.

In this work, we have used a thigh cuff occlusion/release at a single frequency of 0.067 Hz. We found that the phase shifts between deoxy- and oxy-hemoglobin concentrations calculated with the mBLL at the first source-detector separation (~8 mm) differ from those calculated at the third (~18 mm) and sixth (~38 mm) source-detector separations. Since the first channel mostly probes the superficial scalp and skull layers, while the second and the third channels are more sensitive to the brain hemodynamics, these results indicate that the vascular dynamics (blood flow, blood volume), the physiological parameters (capillary and venous transit times etc.), or both are different between the scalp and the brain. For the two-layer model, we have found equal phase shifts (within errors) between oxy- and deoxy-hemoglobin oscillations for the top and bottom layers. However, this observation is not enough to conclude that also the vascular dynamics and physiological parameters are the same for the top and bottom layers. In fact, we remind that CHS makes use of spectra, i.e. of phase shifts and amplitudes ratios between hemoglobin species calculated at different frequencies, therefore the observations we can derive by using only one frequency (as it was done in this work) are not conclusive.

Another comment concerns the apparent discrepancy between the two models used for the calculations of hemoglobin oscillations. One would expect that the hemoglobin oscillations of the top layer retrieved by a two-layer model would reflect only the oscillations of scalp and skull, and should be similar to the oscillations measured by mBLL at the shortest source-detector separations (up to around 1-1.5 cm). On the contrary, this study could not confirm this point and further investigations are needed. One possible explanation is that the hemoglobin oscillations induced by the forcing mechanism have a highly heterogeneous nature and cannot be considered uniform in each head layer (i.e. the absorption changes are not "layered-like"). In these conditions, by using the two-layer model we would most probably obtain a weighted average of the oscillations occurring in different tissue regions probed by different channels.

In summary, this work represents the first step toward the development of depth-resolved CHS, which ultimately can result in a powerful non-invasive optical method for the non-invasive assessment of cerebral perfusion and autoregulation.

ACKNOWLEDGEMENTS

This research is supported by the US National Institutes of Health (Grant no. R01-CA154774).

REFERENCES

Boas, D. A., Jones, S. R., Devor, A., Huppert, T. J., Dale, A. M., 2008. A vascular anatomical network model of the spatio-temporal response to brain activation. *Neuroimage* 40, 1116-1129.

Boashash, B., 1992. Estimating and interpreting the instantaneous frequency of a signal. Part 1: Fundamentals. *Proceedings of IEEE* 80, 520-538.

Buxton, R. B., Frank, L. R., 1997. A model of the coupling between cerebral blood flow and oxygen metabolism during neural stimulation. *Journal of cerebral blood flow & metabolism* 17, 64-72.

Choi, J., Wolf, M., Toronov, V., Wolf, U., Polzonetti, C., Hueber, D., Safonova, L. P., Gupta, R., Michalos, R., Mantulin, W., Gratton, E., 2004. Noninvasive determination of the optical properties of adult brain: near-infrared spectroscopy approach. *Journal of Biomedical Optics* 9: 221-229.

Diamond, S. G., Perdue, K. L., Boas, D. A., 2009. A cerebrovascular response model for functional neuroimaging including cerebral autoregulation. *Mathematical Biosciences* 220, 102-117.

Fantini, S., Franceschini-Fantini, M. A., Maier, J.S., Walker, S.A., Barbieri, B., Gratton, E., 1995. Frequency-domain multichannel optical detector for noninvasive tissue spectroscopy and oximetry. *Optical Engineering* 34, 32-42.

Fantini, S., 2014a. Dynamic model for the tissue concentration and oxygen saturation of hemoglobin in relation to blood volume, flow velocity, and oxygen consumption: Implications for functional neuroimaging and coherent hemodynamics spectroscopy (CHS). *Neuroimage* 85, 202-221.

Fantini, S., 2014b. A new hemodynamic model shows that temporal perturbations of cerebral blood flow and metabolic rate of oxygen cannot be measured individually using functional near-infrared spectroscopy. *Physiological Measurements* 35, N1-N9.

Gagnon, L., Gauthier, C., Hoge, R. D., Lesage, F., Selb, J., Boas, D.A., 2008. Double-layer estimation of intra- and extracerebral hemoglobin concentration with a time-resolved system. *Journal of Biomedical Optics* 13: 054019.

Hallacoglu, B., Sassaroli, A., Fantini, S., 2013. Optical characterization of two-layered turbid media for non-invasive, absolute oximetry in cerebral and extracerebral tissue," *PLoS ONE* 8, e64095.

Huppert, T. J., Allen, M.S., Benav, H., Jones, P. B., Boas, D. A., 2007. A multicompartment vascular model for inferring baseline and functional changes in cerebral oxygen metabolism and arterial dilation. *Journal of cerebral blood flow & metabolism* 27, 1262-1279.

Kainerstorfer, J. M., Sassaroli, A., Tgavalekos, K. T., Fantini, S., 2015. Cerebral autoregulation in the microvasculature measured with near-infrared spectroscopy. *Journal of Cerebral Blood Flow & Metabolism* 35, 959-966.

Liemert, A., Kienle, A., 2010. Light diffusion in a turbid cylinder. II. Layered case. *Optics Express* 18, 9266-9279.

Mandeville, J. B., Marota, J. J., Ayata, C., Zaharchuk, G., Moskowitz, M. A., Rosen, B. R., Weisskoff, R. M., 1999. Evidence of cerebrovascular postarteriole windkessel with delayed compliance. *Journal of Cerebral Blood Flow & Metabolism* 19, 679-689.

Pierro, M., Sassaroli, A., Bergethon, P. R., Ehrenberg, B. L., Fantini, S., 2012. Phase-amplitude investigation of spontaneous low-frequency oscillations of cerebral hemodynamics with near-infrared spectroscopy: A sleep study in human subjects. *Neuroimage*, 63, 1571-1584.

Pierro, M. L., Hallacoglu, B., Sassaroli, A., Kainerstorfer, J.M., Fantini, S., 2014a. Validation of a novel hemodynamic model for coherent hemodynamics spectroscopy (CHS) and functional brain studies with fNIRS and fMRI. *Neuroimage* 85, 222-233.

Pierro, M. L., Kainerstorfer, J. M., Civiletto, A., Wiener, D. E., Sassaroli, A., Hallacoglu, B., Fantini, S., 2014b. Reduced speed of microvascular blood flow in hemodialysis patients versus healthy controls: a coherent hemodynamics spectroscopy study. *Journal of Biomedical Optics* 19, 026005 1-9.

Sassaroli, A., Fantini, S., 2004. Comment on the modified Beer-Lambert law for scattering media. *Physics in Medicine and Biology* 49 N1-N3.

Villringer, A., 2012. The intravascular susceptibility effect and the underlying physiology of fMRI. *Neuroimage* 62, 995-999. PMID: 22305989.